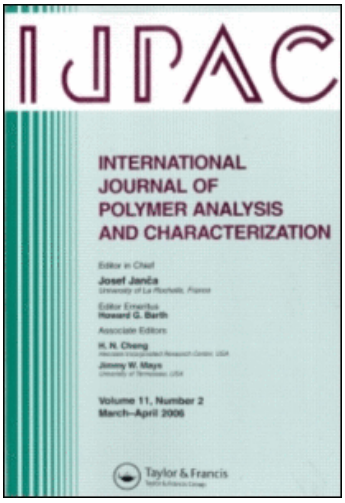

International Journal of Polymer Analysis and Characterization
Publication details, including instructions for authors and subscription information:
http://www.informaworld.com/smpp/title~content=t713646643

Analysis of a Styrene—Butadiene Graft Copolymer by Size Exclusion Chromatography I. Computer Simulation Study for Estimating the Biases Induced by Branching Under Ideal Fractionation and Detection

D. A. Estenoz[a]; J. R. Vega[a]; H. M. Oliva[b]; G. R. Meira[a]
[a] INTEC (Univ. National Del Litoral CONICET), Santa Fe, Argentina [b] Esc. Ing. Química, Univ. Del Zulia, Maracaibo, Venezuela

To cite this Article Estenoz, D. A. , Vega, J. R. , Oliva, H. M. and Meira, G. R.(2001) 'Analysis of a Styrene—Butadiene Graft Copolymer by Size Exclusion Chromatography I. Computer Simulation Study for Estimating the Biases Induced by Branching Under Ideal Fractionation and Detection', International Journal of Polymer Analysis and Characterization, 6: 3, 315 — 337
To link to this Article: DOI: 10.1080/10236660108033950
URL: http://dx.doi.org/10.1080/10236660108033950

Int. J. Polym. Anal. Charact.,
2001 Vol. 6, pp. 315–337
Reprints available directly from the publisher
Photocopying permitted by license only

Analysis of a Styrene–Butadiene Graft Copolymer by Size Exclusion Chromatography

I. Computer Simulation Study for Estimating the Biases Induced by Branching Under Ideal Fractionation and Detection*

D. A. ESTENOZ[a], J. R. VEGA[a], H. M. OLIVA[b] and G. R. MEIRA[a,†]

[a]*INTEC (Univ. Nacional Del Litoral CONICET), Güemes 3450 (3000) Santa Fe, Argentina;* [b]*Esc. Ing. Química, Univ. Del Zulia, Maracaibo, Venezuela*

(Received 12 November 1999; In final form 3 April 2000)

This theoretical work estimates the deviations in the molecular weights distribution (MWD), the degree of branching distribution (DBD), and the chemical composition distribution (CCD) due to branching when a (chromatographically complex) styrene–butadiene graft copolymer is analyzed by ideal size exclusion chromatography (SEC). The copolymer was isolated from a high-impact polystyrene. A novel polymerization model was developed that predicts the MWD, DBD, and CCD for the total copolymer and for each of its different branched topologies. Copolymer topologies are characterized by the number of trifunctional branching points per molecule. To simulate the molecular weight calibrations in SEC, the Zimm–Stockmayer equation was applied to each copolymer topology. Negligible deviations due to branching were found in the MWD and the DBD with respect to the theoretical predictions provided by the polymerization model. In contrast, errors in the CCD are intolerably large and consequently the CCD cannot be estimated by SEC.

Keywords: Size exclusion chromatography; Styrene–butadiene graft copolymer; Computer simulation; High-impact polystyrene

* Presented at the 13th Bratislava International Conference on Polymers, "Separation and Characterization of Macromolecules", July 4–9, 1999.

† Corresponding author.

INTRODUCTION

Ideally, size exclusion chromatography (SEC) fractionates according to hydrodynamic volume. Thus, instantaneous distributions of molecular weights, chemical composition, and degrees of branching are present in the detector cell when a (chromatographically complex) branched copolymer is analyzed. Such instantaneous distributions then induce biases when estimating the molecular weight distribution (MWD), the degree of branching distribution (DBD), and/or the chemical composition distribution (CCD). In a real SEC measurement, other sources of error such as secondary fractionation, axial dispersion, biased measurements, and polymer degradation can be also present, but these problems will not be considered here.

Computer simulation studies of the different processes that operate in SEC can be helpful for separating, understanding, and correcting each of the eventual sources of error. For example, based on samples of known MWDs, Guaita and Chiantore[1] simulated the chromatograms obtained with an on-line viscometer and a differential refractometer to study the effect of the injected sample concentration on parameters such as the Mark–Houwink constants K and α. It was proven that errors in the sample concentration are directly propagated into the average molecular weights and K, but do not affect α or the MWD shape.

Radke *et al.*[2] determined the errors in the number-average molecular weight ($\overline{M}_n$) when a complex copolymer is analyzed in a chromatograph fitted with a differential refractometer and a light-scattering detector. It was proven that accurate estimations of $\overline{M}_n$ are only possible when each chromatogram slice is monodisperse in molecular weights and in composition.

Brun[3] developed theoretical expressions for estimating the MWD and the intrinsic viscosity distribution (IVD) when the chromatograph is fitted with a differential refractometer, a capillary viscometer, and a light-scattering detector. When analyzing a chromatographically complex polymer, the following was observed: (a) to obtain the MWD and the IVD, only the viscometer and light scattering signals are required; and (b) from all three signals, the instantaneous hydrodynamic volume can be obtained.

The graft copolymer that is here investigated had been previously analyzed (both experimentally and theoretically) by Estenoz *et al.*[4] The sample was synthesized in a solution polymerization of styrene (St) in the presence of polybutadiene (PB), to emulate a high-impact polystyrene (HIPS) process.[4] The reaction was carried out at low temperature and at low conversion, therefore no significant cross-linking was present. All HIPS components (i.e., free polystyrene (PS), unreacted PB, and the graft copolymer) were first isolated from each other by solvent extraction, and then analyzed by SEC. The chemical composition was seen to vary little with molecular weight. The grafted St branches were isolated from the graft copolymer by ozonolysis and analyzed by SEC. From the moles of copolymer and of grafted St branches, the number-average number of St branches per copolymer molecule was obtained. The polymerization model developed in Estenoz *et al.*[4] was based on a kinetics involving: chemical initiation, thermal initiation, propagation, termination by combination, transfer to the monomer, transfer to the rubber, and transfer to the solvent. Two types of cross-linking reactions were admitted: (a) H grafting by recombination of two copolymer radicals; and (b) pure rubber cross-linking by termination of two primary rubber radicals. During the prepolymerization, pure rubber cross-linking proved negligible, while H grafting remained moderate. The mathematical model predicted the (bivariate) weight chain-length distribution (WCLD) for the total copolymer; and from such distribution, the (univariate) MWD and CCD were obtained. Theoretical predictions on the DBD of the graft copolymer present in HIPS have never so far been developed.

The polymerization models presented in our first articles on the HIPS process,[5,6] classified the graft copolymer molecules into topologies characterized by two integers: the number of St and butadiene (Bd) chains per molecule. However, due to the impossibility of validating the detailed model predictions, in our later publications (Refs. [4, 7, 8]), only the global copolymer distributions were calculated.

This work theoretically evaluates the errors due to branching when the St–Bd graft copolymer sampled at 16 h in Estenoz *et al.*[4] is analyzed by ideal SEC. To this effect, a mathematical model is developed that simulates the polymerization process and the ideal SEC fractionation.

THE POLYMERIZATION – IDEAL SEC MODEL

The polymerization mechanism of Table I is adopted. It coincides with that of Estenoz *et al.*[4] except for the fact that the copolymer molecules are classified into $1, 2, \ldots$ topologies characterized by a single integer: the number of trifunctional grafting points per molecule r. To represent a copolymer molecule of topology r, with s repetitive units of St and b repetitive units of Bd, the terminology $P_{(r)}(s, b)$ is used. All symbols of Table I are explained in the nomenclature section.

For any given copolymer species, many chemical configurations are possible. This is illustrated in Figure 1 for an hypothetical $P_{(4)}(18, 20)$ molecule. In Figure 1a, a (more normal) T-grafted structure containing a single Bd chain is presented. In Figure 1b, an H graft containing two Bd chains is shown. It is easily seen that the number of trifunctional branching points per molecule r is equal to the total number of St and Bd chains minus 1.

From the kinetics of Table I, a polymerization model is developed (see appendix). The model consists of Eqs. (A.1)–(A.8) and (A.14)–(A.22). Equations (A.1)–(A.8) calculate the main global compositions; Eq. (A.21) calculates the bivariate WCLD for each of the different topologies; and Eq. (A.22) calculates the bivariate WCLD for the total copolymer. The model parameters were adopted identical to those employed in our previous publications (Refs. [6, 4]), and therefore no specific adjustments were implemented. In Estenoz *et al.*[6] most model parameters were directly taken from the literature and only three rate constants had to be adjusted to the measurements within expected literature ranges. For the numerical resolution, a procedure similar to that described in Estenoz *et al.*[4] was applied.

Consider now the ideal chromatography model. The chromatograph is ideal in the sense that: fractionation is strictly by hydrodynamic volume; and exact measurements of the instantaneous average molecular weights, average chemical compositions, and average degrees of branching are available. Only the effect of branching on hydrodynamic volume will be investigated. (The copolymer composition effect is assumed negligible because as it will become clearer below, all copolymer topologies are expected to exhibit similar composition distributions.) Also, the graft copolymer is treated as a branched homopolymer from the point of view of its hydrodynamic

TABLE I Adopted kinetic mechanism

Chemical initiation	$I_2 \xrightarrow{k_d} 2I^{\cdot}$
	$I^{\cdot} + St \xrightarrow{k_{i1}} S_1^{\cdot}$
	$I^{\cdot} + P_{(r)}(s,b) \xrightarrow{k_{i2}} P^{\cdot}_{0_{(r)}}(s,b)$
Thermal initiation	$3\ St \xrightarrow{k_{i0}} 2\ S_1^{\cdot}$
Propagation	$S_n^{\cdot} + St \xrightarrow{k_p} S_{n+1}^{\cdot}$
	$P^{\cdot}_{0_{(r)}}(s,b) + St \xrightarrow{k_{p0}} P^{\cdot}_{1_{(r)}}(s,b)$
	$P^{\cdot}_{n_{(r)}}(s,b) + St \xrightarrow{k_p} P^{\cdot}_{n+1_{(r)}}(s,b)$
Transfer to the monomer	$S_n^{\cdot} + St \xrightarrow{k_{fm}} S_n + S_1^{\cdot}$
	$P^{\cdot}_{m_{(r-1)}}(s-m,b) + St \xrightarrow{k_{fm}} P_{(r)}(s,b) + S_1^{\cdot}$
	$P^{\cdot}_{0_{(r)}}(s,b) + St \xrightarrow{k'_{fm}} P_{(r)}(s,b) + S_1^{\cdot}$
Transfer to the PB or the copolymer	$S_n^{\cdot} + P_{(r)}(s,b) \xrightarrow{k_{fs}} S_n + P^{\cdot}_{0_{(r)}}(s,b)$
	$P^{\cdot}_{m_{(r-1)}}(s-m,b) + P_{(r_1)}(s_1,b_1) \xrightarrow{k_{fs}} P_{(r)}(s,b) + P^{\cdot}_{0_{(r_1)}}(s_1,b_1)$
Transfer to the solvent	$S_n^{\cdot} + T \xrightarrow{k_{ft}} S_1^{\cdot} + S_n$
	$P^{\cdot}_{m_{(r-1)}}(s-m,b) + T \xrightarrow{k_{ft}} S_1^{\cdot} + P_{(r)}(s,b)$
	$P^{\cdot}_{0_{(r)}}(s,b) + T \xrightarrow{k'_{ft}} S_1^{\cdot} + P_{(r)}(s,b)$
Termination by combination	$S_n^{\cdot} + S_m^{\cdot} \xrightarrow{k_{tc}} S_{n+m}$
	$P^{\cdot}_{m-n_{(r-1)}}(s-m,b) + S_n^{\cdot} \xrightarrow{k_{tc}} P_{(r)}(s,b)$
	$P^{\cdot}_{m-n_{(r-r_1-1)}}(s-s_1-m,b-b_1) + P^{\cdot}_{n_{(r_1-1)}}(s_1,b_1) \xrightarrow{k_{tc}} P_{(r)}(s,b) \quad r > (r_1-1)$
	$P^{\cdot}_{0_{(r-r_1-1)}}(s-s_1-n,b-b_1) + P^{\cdot}_{n_{(r_1)}}(s_1,b_1) \xrightarrow{k''_{tc}} P_{(r)}(s,b) \quad r > (r_1-1)$
	$P^{\cdot}_{0_{(r-1)}}(s-n,b) + S_n^{\cdot} \xrightarrow{k''_{tc}} P_{(r)}(s,b)$

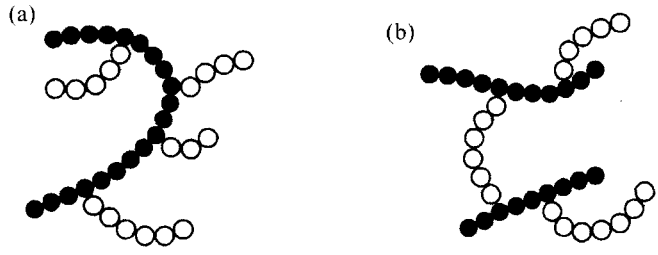

FIGURE 1 Two possible configurations of a St–Bd graft copolymer molecule with $r=4$ trifunctional branching points, $s=18$ St units (white circles), and $b=20$ Bd units (black circles).

volume behavior. This is justified as follows: good solvents are used in SEC, thus reducing the intramolecular interactions between St and the Bd chains; and the solubility parameters of PS and PB are close to each other, thus indicating a low interaction between the different graft copolymer chains.

For flexible molecules and for a given molecular weight, the g branching parameter is defined as the ratio between the mean-square-radius of gyration of a branched molecule and the mean-square-radius of gyration of an homologue linear molecule. For branched homopolymers containing trifunctional branching points, the Zimm–Stockmayer expression[9] relates g (at any given molecular weight) with the number-average number of trifunctional branching points per molecule. In this work, we shall apply such expression, but to each individual copolymer topology r, providing

$$g_r = \left[\left(1+\frac{r}{7}\right)^{1/2} + \frac{4r}{9\pi}\right]^{-1/2} \leq 1; \quad (M_b = M_l); \quad (r = 0,1,2,\ldots) \quad (1)$$

where g_r indicates the g value of topology r and M_b, M_l are respectively the molecular weights of branched and linear molecules. Note the following: for a linear block copolymer, $r=0$ and $g_0 = 1$; and for any given topology, g_r is a constant for all M values, irrespectively of the copolymer configuration (Fig. 1). Similarly, from the g' branching parameter based on the hydrodynamic volume ratio, a g'_r parameter may be defined that is applied to each copolymer topology,

yielding

$$g'_r \equiv \frac{[\eta]_r}{[\eta]_l} = \frac{[\eta]_r}{KM_l^{\alpha}}; \quad (M_b = M_l); \quad (r = 0, 1, 2, \ldots) \tag{2}$$

where $[\eta]_r$ is the intrinsic viscosity of topology r, $[\eta]_l$ is the intrinsic viscosity of a linear homologue, and K and α are the Mark–Houwink constants of a linear homologue. For the linear homologue, we shall here adopt a linear diblock copolymer of similar composition (and molecular weights) as the analyzed copolymer. The reason for this is mainly practical: reliable information on the Mark–Houwink constants is only available for linear diblock copolymers. Both branching parameters are interrelated through [10]

$$g'_r = g_r^{\varepsilon}; \quad (M_b = M_l); \quad (r = 0, 1, 2, \ldots) \tag{3}$$

where ε is an empirical exponent. This exponent has been generally assumed a constant for a given polymer-solvent system, but more recently it has been considered as molecular weight dependent. [11] If ε is adopted a constant, then (for any given topology) g'_r will be also independent of M. However, note that for the global copolymer, the instantaneous $g(V)$ and $g'(V)$ are not constant, since the relative amount of the different topologies vary along elution volume.

For a given solvent and temperature, the universal calibration concept is based on the assumption that the product $[\eta]\,M$ is proportional to the hydrodynamic volume, irrespectively of the copolymer topology. Strictly speaking however, such assumption only holds for polymer solutions in theta conditions. Since good solvents are used in SEC, deviations of the universal calibration are to be expected, and their quantification is still a matter of investigation. [3] Thus, in this work we shall assume that all copolymer species are ideally fractionated according to an independently obtained universal calibration: $\log([\eta]\,M) = A - B\,V$, where A and B are constants. From the linear universal calibration and Eqs. (2)–(3), the following expression for the individual molecular weight calibration for each copolymer topology is obtained:

$$\log M = \frac{A - \log(g_r^{\varepsilon} K)}{\alpha + 1} - \frac{B}{\alpha + 1} V; \quad (r = 0, 1, 2, \ldots) \tag{4}$$

Equation (4) indicates that all individual calibrations exhibit a common slope $[-B/(\alpha+1)]$, and a varying y-intercept $[A - \log(g_r^{\epsilon}K)]/[\alpha+1]$. Also note that a one-to-one relationship between M and V has be established for any given topology r.

SIMULATION RESULTS

The polymerization described in Estenoz *et al.*[4] is here reconsidered. It consisted of a batch polymerization of St in the presence of medium-*cis*-1,4 PB carried out at 70°C in a dilute toluene solution, and using *tert*-butyl peroctoate as initiator. The analyzed polymer was sampled at 16 h, and the monomer conversion was 17.6%. Its global St mass fraction was 44%, and the average number of trifunctional branching points per molecule was approximately 2.[4] This last result coincides with a prediction by Fischer and Hellmann[12] for a similar solution polymerization at approximately the same conversion.

Consider first the polymerization model predictions of Figures 2, 3a, 4a and 5a, and in the first rows of Table II. Figure 2 illustrates the bivariate WCLDs for the total copolymer and for some of the produced topologies. The univariate MWD, DBD, and CCD for the total copolymer and for the 16 calculated topologies were obtained from their bivariate WCLDs.

The theoretical DBD as provided by the polymerization model is strictly discrete, therefore its distribution is represented by the mass G vs the (integer) number of trifunctional branching points per molecule r. All other distributions are represented as continuous functions, and therefore their ordinates represent the derivative of G with respect to the variable presented in the horizontal axis. In the continuous representations of the MWD, DBD, and CCD, the "distributed" variables are $\log M$, r, and p, respectively. Note the following: in all continuous distributions, the area under the curves are proportional to the polymer mass at the given conversion; $\log M$ rather than M was selected for the MWD in order that its shape appears similar to that of the mass chromatogram; and in the "continuous" DBD, r is a real variable instead of an integer. The univariate "theoretical" MWD, DBD, and CCD as predicted by the polymerization model are presented in narrow tracings in Figures 3a, 4a and 5a.

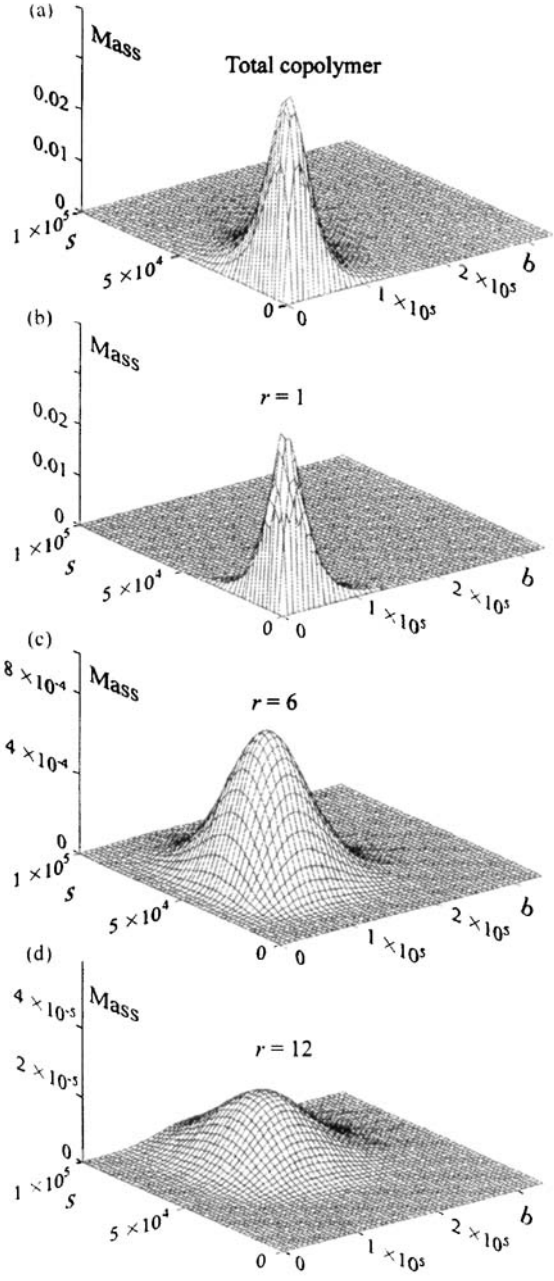

FIGURE 2 The analyzed copolymer. Bivariate WCLDs for the total copolymer (a), and for topologies $r = 1$, 6, and 12 (b–d).

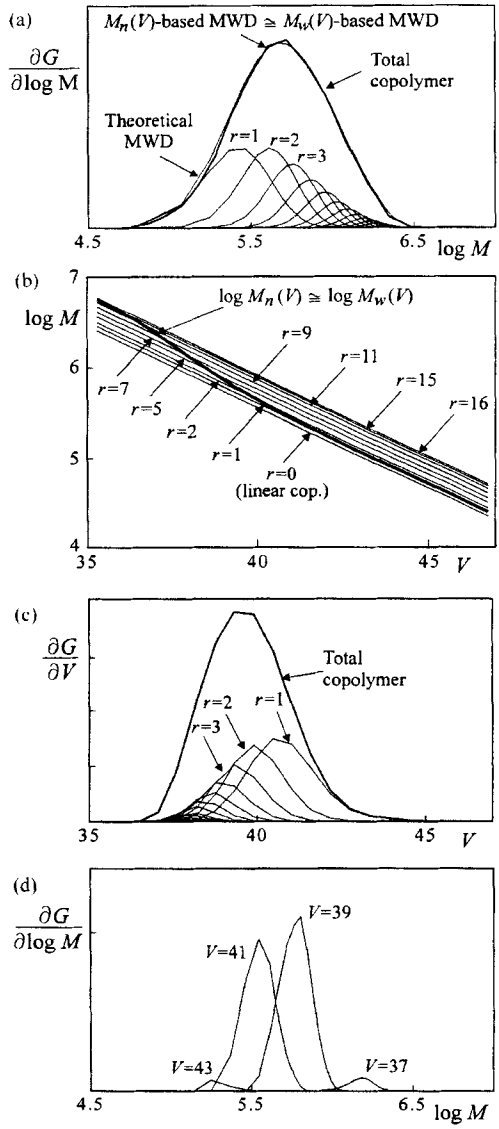

FIGURE 3 The analyzed copolymer. (a) The MWDs for the total copolymer and for the main topologies as predicted by the polymerization model (theoretical MWD, narrow lines) are compared with two chromatographically recuperated MWDs (bold lines). (b) Molecular weight calibrations for each different copolymer topology (narrow lines) and for the total copolymer (bold line). (c) Mass chromatograms. (d) Instantaneous MWDs at four elution volumes.

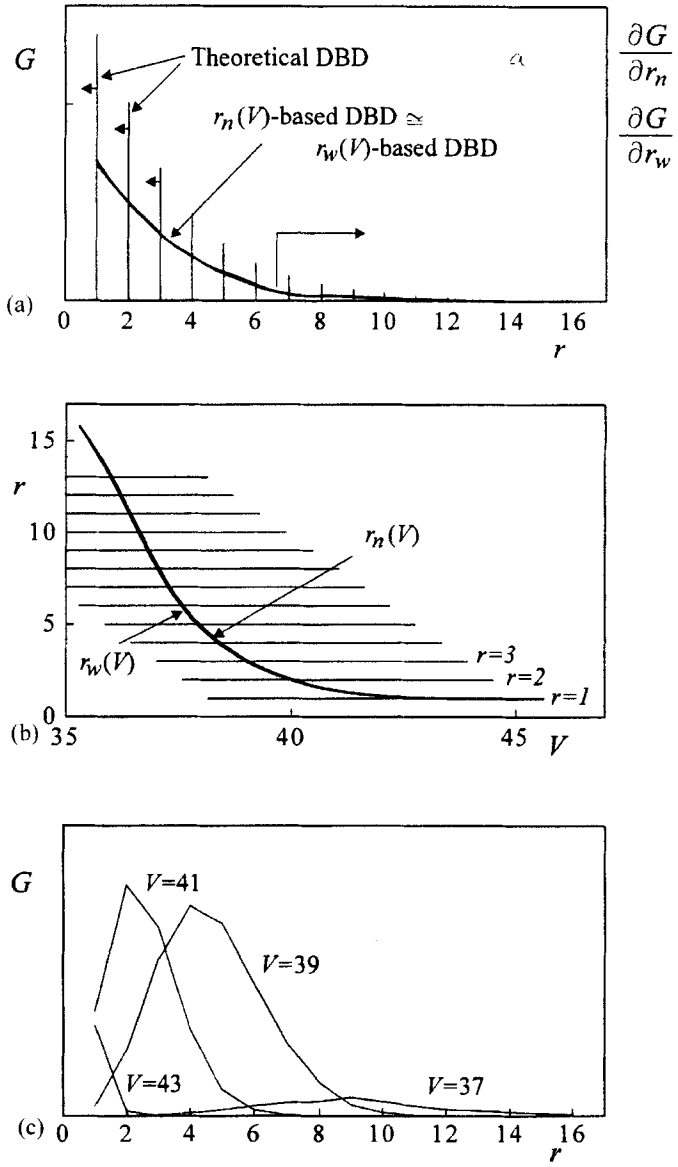

FIGURE 4 The analyzed copolymer. (a) The theoretical (discrete) DBD for the total copolymer (narrow lines) as predicted by the polymerization model is compared with two (continuous) "chromatographic" DBDs (bold lines). (b) Theoretical (discrete) calibrations and (continuous) measurements of the average degrees of branching. (c) Instantaneous DBDs at four elution volumes.

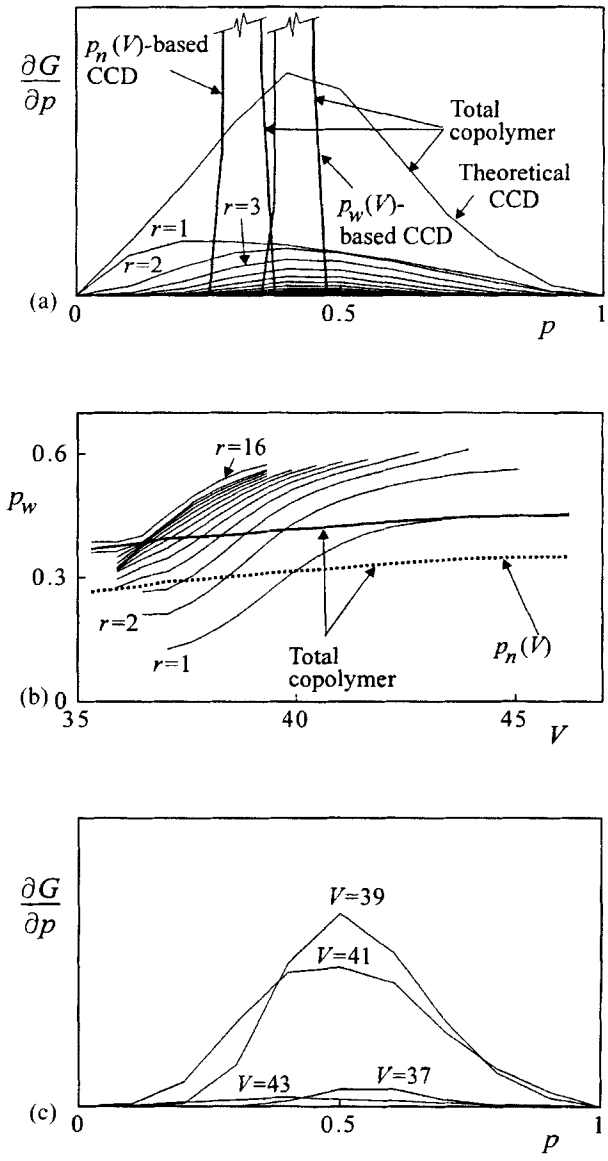

FIGURE 5 The analyzed copolymer. (a) The theoretical CCDs for the total copolymer and for the main topologies as predicted by the polymerization model (narrow line) are compared with two chromatographically-recuperated CCDs (bold line). (b) Instantaneous St mass fraction for the different topologies (narrow line) and for the total copolymer (bold line). Instantaneous St molar fraction for the total copolymer (dotted line). (c) Instantaneous CCDs at four elution volumes.

TABLE II Global characteristics of the analyzed St–Bd graft copolymer. The distribution averages as predicted by the polymerization model are compared with the "chromatographic" predictions obtained in ideal SEC

	Global estimates		
Distribution	*Number average*	*Weight average*	*Polydispersity*
Theoretical MWD	355000	599000	1.69
Theoretical DBD	1.99	3.02	1.52
Theoretical CCD	0.34	0.44	1.29
$M_n(V)$-based MWD	356000	587000	1.65
$M_w(V)$-based MWD	366000	598000	1.63
MWD for $r=0$ calibr.	245000	387000	1.58
$r_n(V)$-based DBD	1.99	2.99	1.50
$r_w(V)$-based DBD	2.01	3.02	1.50
$p_n(V)$-based CCD	0.33	0.34	1.03
$p_w(V)$-based CCD	0.43	0.44	1.02

The MWDs are represented in Figure 3a. As expected, higher topologies exhibit increased average molecular weights. The theoretical DBD is discrete, since only integers of r are possible (Fig. 4a). At the investigated conversion, the first topology is the most abundant. At higher conversions, the most abundant topologies become $r=2$, $r=3$, *etc.* The CCDs for the total copolymer and for the individual topologies are presented in Figure 5a. As r increases, the CCDs become somewhat narrower, but their averages remain relatively constant. This is because: (a) the grafting probability of a Bd chain is directly proportional to its molar mass, and therefore the average number of Bd units between trifunctional branching points is relatively constant along the topologies, varying from 2200 for $r=1$ to 1700 for $r=16$; and (b) the average chain lengths of the grafted St branches vary little along the isothermal reaction.[4]

Consider now the SEC model predictions. We shall here simulate the SEC conditions of Ref. [13]. The carrier solvent was tetrahydrofuran, and the analysis was performed at 25°C. The universal calibration constants were:[13] $A=18.09$ and $B=0.3041$. The Mark–Houwink constants used are: $K=3.2\times10^{-4}$ dL/g and $\alpha=0.693$. These values were suggested by Kraus and Stacy[14] for a linear diblock St–Bd copolymer with an average St mass fraction of 40%, which is close to the composition of the analyzed polymer. Also, the given values were checked by interpolation (with the chemical composition) between reported Mark–Houwink constants for linear

PS and PB homopolymers (Refs. [14–19]). The exponent of Eq. (3) used was $\varepsilon = 2$. This value was estimated in the second part of this series[13] from SEC-viscometry measurements combined with theoretical predictions on the expected $g'(M)$ functions. Three St–Bd graft copolymer samples were investigated in Ref. [13], and the 16 h sample is the subject of the present work.

In Figure 3b, the calibrations for the different copolymer topologies and for the linear homologue are shown as a narrow tracing. For the copolymer topologies, Eq. (4) was applied. For the linear block copolymer, the calibration was calculated from $\log(\mathrm{K}\, M^{\alpha+1}) = \mathrm{A} - \mathrm{B}\, V$. Note that according to our model, one-to-one relationships can be established between $\log M$ and V for any of the different topologies and for the linear copolymer. By combining the MWD of each topology with its corresponding calibration, the topology chromatograms of Figure 3c were obtained.

By addition of the individual topology chromatograms, the mass chromatogram of the total copolymer was calculated (Fig. 3c). From the mass chromatograms of each individual topology, the instantaneous MWDs in the detector cell were determined (Fig. 3d). Also, from the instantaneous MWDs, the instantaneous averages $M_n(V)$ and $M_w(V)$ were obtained. When represented with a logarithmic vertical axis, these functions constitute the ad hoc calibrations $\log M_n(V)$ and $\log M_w(V)$ that would be obtained from ideal molar mass detectors (Fig. 3b). The instantaneous MWDs are quite narrow (Fig. 3d), and the maximum instantaneous polydispersity $M_w(V)/M_n(V)$ is 1.007. For this reason, the mentioned ad hoc calibrations are practically overlapped (Fig. 3b).

From the total copolymer mass chromatogram of Figure 3c and the calibration $\log M_n(V)$ of Figure 3b, the M_n-based MWD of Figure 3a was recuperated. Similarly, the M_w-based MWD of Figure 3a was obtained. These "chromatographic" MWDs are practically overlapped with the original MWD. The observed differences are due to numerical errors introduced when working with discrete functions. As it is seen in Table II, the M_n-based MWD exactly recuperates $\overline{M}_n$, but (very slightly) underestimates $\overline{M}_w$ while the M_w-based MWD exactly recuperates $\overline{M}_w$, but (very slightly) overestimates $\overline{M}_n$. Ideal sensors produce unbiased estimates of the instantaneous averages and masses being measured. For this reason, the global averages whose

instantaneous values are being measured also result unbiased. For comparison, the average molecular weights obtained when adopting the linear block copolymer calibration indicated with $r=0$ in Figure 3b, are also shown in Table II. In this case, both $\overline{M}_n$ and $\overline{M}_w$ are grossly underestimated. Also, the polydispersity is lower than the theoretical value of 1.69 because a mass chromatogram produced by mixture of branched species is narrower than the mass chromatogram of an identical MWD, but of linear molecules.

Assume now that ideal sensors were available for the instantaneous number- and weight-average degrees of grafting $r_n(V)$ and $r_w(V)$. In Figure 4b, such ideal measurements are compared with the individual (horizontal) calibrations $r(V)$ of each copolymer topology. In Figure 4c, the instantaneous DBDs at four elution volumes, are represented. Such instantaneous distributions are strictly discrete, with values at integers of r only, but are shown with continuous tracings to simplify the representation. From the total mass chromatogram of Figure 3c and $r_n(V)$, the $r_n(V)$-based DBD of Figure 4a was obtained. Similarly, the $r_w(V)$-based DBD was produced (Fig. 4a). Both "chromatographic" DBDs are practically superimposed. For this reason, the global averages are close to each other, and also close to the theoretical values (Tab. II).

Finally, consider the "chromatographic" determination of the CCD. Let the instantaneous molar and weight fraction of St in the copolymer be set to $p_n(V)$ and $p_w(V)$, respectively. In Figure 5b, the $p_w(V)$ and $p_n(V)$ functions for the total copolymer and the $p_w(V)$ functions for the individual topologies are presented. $p_w(V)$ is quite constant for the total copolymer, but show larger variations for the individual topologies. In Figure 5c, it is seen that the instantaneous CCDs are broad, and their averages vary little with elution volume. For this reason, the $p_n(V)$-based and the $p_w(V)$-based CCDs both result erroneously narrow (Fig. 5a). As before, the global averages whose instantaneous values are not being measured differ considerably from their theoretical values (Tab. II). (In effect, $p_n(V)$ produces a correct global number-average St mass fraction but underestimates the weight average, while $p_w(V)$ produces a correct global weight average but overestimates the number average.) Thus, for both hypothetical detectors, the composition polydispersity is greatly underestimated (Tab. II). (In a recent article,[20] the CCD of a graft copolymer was

estimated by SEC coupled with a differential refractometer and low-angle light scattering detector, but in this case two good solvents, toluene and tetrahydrofuran, had to be used successively.)

To investigate the effect of choosing a different ε exponent in Eq. (3), all computer simulations were repeated, but adopting $\varepsilon = 0.5$ (i.e., the lowest reported value). Almost coincident distributions with respect to the base case of $\varepsilon = 2$ were recuperated. This is to be expected, since according to our ideal SEC model, ε strongly affects the viscosity measurements but has practically no influence on the SEC fractionation.

CONCLUSIONS

In this work, the ideal SEC fractionation of a St–Bd graft copolymer was simulated, with the aim of evaluating the errors in the distribution estimates due to branching. The instantaneous MWDs and DBDs are narrow, and their averages vary monotonically with elution volume. Thus, estimation errors in the mentioned distributions are low. In contrast, the instantaneous CCDs are broad, and their averages vary little with elution volume. For this reason, the CCD cannot be determined by SEC.

Distribution estimates were seen to be quite unaffected by the ε exponent of Eq. (3). This is rather fortunate, since it makes it possible to simulate representative SEC fractionations even when ε is unknown.

Acknowledgments

We thank CONICET, SECYT, Universidad Nacional del Litoral, Universidad del Zulia, CONDES-LUZ, and CONICET (Argentina), CONICIT (Venezuela) agreement for the financial support.

NOMENCLATURE

A, B	y-intercept and slope of the (linear) universal molecular weight calibration, respectively
b	number of Bd repetitive units
B*	unreacted Bd unit
$B^*_{(r)}(s, b)$	unreacted Bd unit of $P_{(r)}(s, b)$

f	initiator efficiency
G	mass
g_r	branching parameter defined in Eq. (1), and applied to topology r
g'_r	branching parameter defined in Eq. (2), and applied to topology r
$\mathrm{I}^{\cdot}$	primary initiator radical
I_2	chemical initiator
k_d	initiator decomposition rate constant
k_{fg}	rate constant of chain transfer to the rubber
k_{fm}, k'_{fm}	rate constants of chain transfer to the monomer
k_{ft}, k'_{ft}	rate constants of chain transfer to the solvent
k_{i0}	rate constant of thermal monomer initiation
k_{i1}, k_{i2}, k_{p0}	initiation rate constants
k_p	propagation rate constant
k_{tc}, k''_{tc}	rate constants of recombination termination
K	Mark–Houwink constant
M	molecular weight
M_{Bd}, M_{St}	molecular weights of Bd and St units (54.06 g/mol and 104.15 g/mol, respectively)
$M_n(V)$	instantaneous number-average molecular weight
$M_w(V)$	instantaneous weight-average molecular weight
p	weight fraction of St in the copolymer
$p_n(V)$	instantaneous number-average St mass fraction
$p_w(V)$	instantaneous weight-average St mass fraction
$\mathrm{P}_{(r)}(s,b)$	copolymer molecule of topology r, with s repetitive units of St, and b repetitive units of Bd (the unreacted PB is also assumed a special copolymer with $r=s=0$)
$\mathrm{P}^{\cdot}$	generic copolymer radical
$\mathrm{P}^{\cdot}_0$	generic primary rubber radical
$\mathrm{P}^{\cdot}_{0(r)}(s,b)$	primary rubber radical
$\mathrm{P}^{\cdot}_{n(r)}(s,b)$	radical produced from $\mathrm{P}^{\cdot}_{0(r)}(s,b)$
r	number of trifunctional grafting points per molecule
$r_n(V)$	instantaneous number-average number of trifunctional points per molecule
$r_w(V)$	instantaneous weight-average number of trifunctional points per molecule
R_p	global rate of St consumption

s	number of St repetitive units
S_n	PS molecule of chain length n
$S^{\cdot}$	St radical
$S_n^{\cdot}$	PS homoradical of chain length n
T	solvent
t	time, s
V	elution volume
V_R	reaction volume
[ ]	molar concentration

Greek Letters

α	Mark-Houwink constant
$\beta, \varphi, \gamma, \theta, \tau, \tau_1$	dimensionless kinetic parameters
ε	branching exponent defined in Eq. (3)

Subscripts

l	linear molecule
b	branched molecule

References

[1] M. Guaita and O. Chiantore (1993). *J. Liq. Chromatogr.*, **16**, 633.
[2] W. Radke, P. Simon and A. Müller (1996). *Macromolecules*, **29**, 4926.
[3] Y. Brun (1998). *J. Liq. Chromatogr. and Rel. Technol.*, **21**, 1979.
[4] D. A. Estenoz, I. M. González, H. M. Oliva and G. R. Meira (1999). *J. Appl. Polym. Sci.*, **74**, 1950.
[5] D. A. Estenoz and G. R. Meira (1993). *J. Appl. Polym. Sci.*, **50**, 1081.
[6] D. A. Estenoz, E. Valdez, H. M. Oliva and G. R. Meira (1996a). *J. Appl. Polym. Sci.*, **59**, 861.
[7] D. A. Estenoz, G. P. Leal, Y. R. López, H. M. Oliva and G. R. Meira (1996b). *J. Appl. Polym. Sci.*, **62**, 917.
[8] D. A. Estenoz, N. Gómez, H. M. Oliva and G. R. Meira (1998). *AIChE J.*, **44**, 427.
[9] B. H. Zimm and W. H. Stockmayer (1949). *J. Chem. Phys.*, **17**, 1301.
[10] J. W. Mays and N. Hadjichristidis (1991). In: *Modern Methods of Polymer Characterization*, H. Barth and J. Mays (Eds.), J. Wiley & Sons.
[11] P. Tackx and J. C. Tacx (1998). *Polymer*, **39**, 3109.
[12] M. Fischer and G. P. Hellmann (1996). *Macromolecules*, **29**, 2498.
[13] J. R. Vega, D. A. Estenoz, H. M. Oliva and G. R. Meira (2000). *Int. J. Polym. Anal. Charact.*
[14] G. Kraus and C. J. Stacy (1972). *J. Appl. Polym. Sci.*, A-2, **10**, 657.
[15] L. H. Tung (1979). *J. Appl. Polym. Sci.*, **24**, 953.

[16] M. R. Ambler (1980). *J. Appl. Polym. Sci.*, **25**, 901.
[17] A. Rudin (1982). In: "*The Elements of Polymer Science and Engineering*", Academic Press, Inc.
[18] M. A. Hanney, J. E. Armonas and L. Rosen (1987). *ACS Symp. Ser.*, No. 352.
[19] J. Brandrup and E. H. Immergut (Eds.) (1989). *Polymer Handbook*, 3rd edn., Wiley, New York.
[20] L. Mrkvicková (1999). *J. Liq. Chrom. and Rel. Technol.*, **22**, 205.

APPENDIX

Polymerization Model

Consider first a global mass balance which does not include the accumulated copolymer. Call V_R the reaction volume, B* any repeating unit of Bd in the copolymer or in the PB containing an unreacted double bond, and $[S^{\cdot}]$, $[P_0^{\cdot}]$, and $[P^{\cdot}]$ the global concentrations of $S_n^{\cdot}$, $P_{0(r)}^{\cdot}(s,b)$, and $P_{n(r)}^{\cdot}(s,b)$, respectively. These last concentrations are obtained as follows: $[S^{\cdot}] = \sum_n [S_n^{\cdot}]$; $[P_0^{\cdot}] = \sum_r \sum_s \sum_b [P_{0(r)}^{\cdot}(s,b)]$; and $[P^{\cdot}] = \sum_r \sum_s \sum_b \sum_n [P_{n(r)}^{\cdot}(s,b)]$. From the kinetics of Table I, the following may be written:

$$\frac{d}{dt}\{[I_2]V_R\} = -k_d[I_2]V_R \tag{A.1}$$

$$\frac{d}{dt}\{[St]V_R\} = -k_p([S^{\cdot}] + [P^{\cdot}])[St]V_R \tag{A.2}$$

$$\frac{d}{dt}\{[T]V_R\} = -\{k_{ft}([S^{\cdot}] + [P^{\cdot}]) + k'_{ft}[P_0^{\cdot}]\}[T]V_R \tag{A.3}$$

$$\frac{d}{dt}\{[B^*]V_R\} = -\{k_{i2}[I^{\cdot}] + k_{fg}([S^{\cdot}] + [P^{\cdot}])\}[B^*]V_R + \{k'_{fm}[St] + k'_{ft}[T]\}[P_0^{\cdot}]V_R \tag{A.4}$$

$$\frac{d}{dt}\{[I^{\cdot}]V_R\} = \{2fk_d[I_2] - (k_{i1}[St] + k_{i2}[B^*])[I^{\cdot}]\}V_R \cong 0 \tag{A.5}$$

$$\frac{d}{dt}\{[S^{\cdot}]V_R\} = k_{i1}[St][I^{\cdot}]V_R + 2k_{i0}[St]^3V_R + (k'_{fm}[St] + k'_{ft}[T])[P_0^{\cdot}]V_R + (k_{fm}[St] + k_{ft}[T])[P^{\cdot}]V_R - \{k_{fg}[B^*] + k''_{tc}[P_0^{\cdot}] + k_{tc}([S^{\cdot}] + [P^{\cdot}])\}[S^{\cdot}]V_R \cong 0 \tag{A.6}$$

$$\frac{d}{dt}\{[P^{\cdot}]V_R\} = k_{p0}[St][P_0^{\cdot}]V_R - k_{fm}[St][P^{\cdot}]V_R - \{k_{ft}[T] + k_{fg}[B^*] + k''_{tc}[P_0^{\cdot}] + k_{tc}([S^{\cdot}] + [P^{\cdot}])\}[P^{\cdot}]V_R \cong 0 \tag{A.7}$$

$$\frac{d}{dt}\{[P_0^{\cdot}]V_R\} = \{k_{i2}[I^{\cdot}] + k_{fg}([S^{\cdot}] + [P^{\cdot}])\}[B^*]V_R - \{k_{p0}[St] + k'_{fm}[St] + k'_{ft}[T] + k''_{tc}([S^{\cdot}] + [P^{\cdot}])\}[P_0^{\cdot}]V_R \cong 0 \tag{A.8}$$

Equations (A.1)–(A.8) may be simultaneously solved to obtain the concentration of the main reagents and global radicals.

Consider now the detailed mass balance for every possible copolymer radical. From the kinetic mechanism and adopting the pseudo steady-state assumption, the following may be written:

$$\frac{d}{dt}\{[P^{\cdot}_{0(r)}(s,b)]V_R\} = \{k_{i2}[I^{\cdot}] + k_{fg}([S^{\cdot}] + [P^{\cdot}])\}[B^*_{(r)}(s,b)]V_R - \{k_{p0}[St] + k'_{fm}[St] + k'_{ft}[T] + k''_{tc}([S^{\cdot}] + [P^{\cdot}])\}[P^{\cdot}_{0(r)}(s,b)]V_R \cong 0 \qquad r,s = 0,1,2,\ldots; \quad b = 1,2,3,\ldots \tag{A.9}$$

$$\frac{d}{dt}\{[P^{\cdot}_{1(r)}(s,b)]V_R\} = k_{p0}[St][P^{\cdot}_{0(r)}(s,b)]V_R - (k_p + k_{fm})[St][P^{\cdot}_{1(r)}(s,b)]V_R - \{k_{ft}[T] + k_{fg}[B^*] + k_{tc}([S^{\cdot}] + [P^{\cdot}])\}[P^{\cdot}_{1(r)}(s,b)]V_R \cong 0 \qquad r,s = 0,1,2,\ldots; \quad b = 1,2,3,\ldots \tag{A.10}$$

$$\frac{d}{dt}\{[P^{\cdot}_{n(r)}(s,b)]V_R\} = k_p[St][P^{\cdot}_{n-1(r)}(s,b)]V_R - (k_p + k_{fm})[St][P^{\cdot}_{n(r)}(s,b)]V_R - \{k_{ft}[T] + k_{fg}[B^*] + k''_{tc}[P_0^{\cdot}] + k_{tc}([S^{\cdot}] + [P^{\cdot}])\}[P^{\cdot}_{n(r)}(s,b)]V_R \cong 0 \qquad r,s = 0,1,2,\ldots; \quad b = 1,2,3,\ldots \tag{A.11}$$

where $B^*_{(r)}(s,b)$ is any unreacted Bd unit of $P_{(r)}(s,b)$. Comparing Eqs. (A.8) and (A.9), one finds

$$\frac{[P^{\cdot}_{0(r)}(s,b)]}{[P_0^{\cdot}]} = \frac{[B^*_{(r)}(s,b)]}{[B^*]}; \quad r,s = 0,1,2\ldots; \quad b = 1,2,3\ldots \tag{A.12}$$

The bivariate WCLD for each copolymer topology can be obtained from the following mass balance:

$$\frac{d}{dt}\{[\mathrm{P}_{(r)}(s,b)](sM_{St}+bM_{Bd})V_R\} = T_1+T_2+T_3+T_4; \qquad r=0,1,2,\ldots; \quad s,b=1,2,3,\ldots \tag{A.13a}$$

with

$$T_1 = -[\mathrm{B}^*_{(r)}(s,b)]\{k_{i2}[\mathrm{I}^{\cdot}]+k_{fg}([\mathrm{S}^{\cdot}]+[\mathrm{P}^{\cdot}])\}(sM_{St}+bM_{Bd})V_R \tag{A.13b}$$

$$T_2 = \Bigg\{(k_{fm}[\mathrm{St}]+k_{ft}[T]+[k_{fg}\mathrm{B}^*])\sum_{m=1}^{s}[\mathrm{P}^{\cdot}_{m(r-1)}(s-m,b)] + k_{tc}\sum_{m=2}^{s}\sum_{n=1}^{m-1}[\mathrm{P}^{\cdot}_{n(r-1)}(s-m,b)][\mathrm{S}^{\cdot}_{m-n}] + k''_{tc}\sum_{m=1}^{s}[\mathrm{P}^{\cdot}_{0(r-1)}(s-m,b)][\mathrm{S}^{\cdot}_{m}]\Bigg\}(sM_{St}+bM_{Bd})V_R \tag{A.13c}$$

$$T_3 = \Bigg\{\frac{k_{tc}}{2}\sum_{r_1=1}^{r-1}\sum_{b_1=1}^{b-1}\sum_{s_1+m=2}^{s}\sum_{n=1}^{m-1}[\mathrm{P}^{\cdot}_{m-n(r-r_1-1)}(s-s_1,b-b_1)][\mathrm{P}^{\cdot}_{n(r_1-1)}(s_1,b_1)] + \sum_{r_1=1}^{r-1}\sum_{b_1=1}^{b-1}\sum_{s_1+m=2}^{s}k''_{tc}[\mathrm{P}^{\cdot}_{m(r-r_1-1)}(s-s_1-m,b-b)] [\mathrm{P}^{\cdot}_{0(r_1-1)}(s_1,b_1)]\Bigg\}(sM_{St}+bM_{Bd})V_R \tag{A.13d}$$

$$T_4 = \{k'_{fm}[\mathrm{St}]+k'_{ft}[T]\}[\mathrm{P}^{\cdot}_{0(r)}(s,b)](sM_{St}+bM_{Bd})V_R \tag{A.13e}$$

where T_1 represents the rate of disappearance of $\mathrm{P}_{(r)}(s,b)$ by generation of $\mathrm{P}^{\cdot}_{0(r)}(s,b)$, T_2 represents the rate of generation of $\mathrm{P}_{(r)}(s,b)$ by grafting of a new T branch of length m onto a $\mathrm{P}_{(r)}(s-m,b)$ species, T_3 represents the rate of generation of $\mathrm{P}_{(r)}(s,b)$ by recombination of $\mathrm{P}_{(r-r_1-1)}(s-s_1-m,b-b_1)$ and $\mathrm{P}_{(r_1-1)}(s-s_1,b-b_1)$ through a new H branch of length m, and T_4 represents the rate of regeneration of $\mathrm{P}_{(r)}(s,b)$ by deactivation of primary $\mathrm{P}^{\cdot}_{0(r)}(s,b)$ radicals.

As in Estenoz *et al.*[4] the global rate of St consumption (R_p) is obtained from

$$R_p = k_p([S^{\cdot}] + [P^{\cdot}])[St] \tag{A.14}$$

Also, the following dimensionless parameters are defined:

$$\varphi = \frac{[S^{\cdot}]}{[S^{\cdot}] + [P^{\cdot}]} \tag{A.15}$$

$$\theta = \tau + \beta \tag{A.16}$$

$$\tau = \frac{k_{fm}}{k_p} + \frac{k_{ft}[T]}{(k_p[St])} + \frac{k_{fg}[B^*]}{(k_p[St])} + \gamma\tau_1 \tag{A.17}$$

$$\beta = \frac{k_{tc}R_p}{(k_p[St])^2} \tag{A.18}$$

$$\gamma = \frac{[P_0^{\cdot}]}{[S^{\cdot}] + [P^{\cdot}]} \tag{A.19}$$

$$\tau_1 = \frac{k_{tc}''R_p}{(k_p[St])^2} \tag{A.20}$$

Following a treatment similar to that of Estenoz *et al.*[4] Eqs. (A.7)–(A.12) and (A.14)–(A.20) may be introduced into Eqs. (A.13), to obtain the WCLD of each copolymer topology $P_{(r)}(s, b)$

$$\begin{aligned}
&\frac{d}{dt}\{[P_{(r)}(s,b)](sM_{st} + bM_{Bd})V_R\} \\
&\quad = -\left\{\left[R_pV_R(1-\varphi)\left(\tau - \gamma\tau_1 + \beta\varphi + \frac{\gamma\tau_1\varphi}{1-\varphi}\right)\right]\right. \\
&\qquad \left. + [R_pV_R(1-\varphi)(\beta(1-\varphi) + 2\gamma\tau_1)]\right\} \\
&\qquad \times \frac{[B^*_{(r)}(s,b)]}{[B^*]} \times (sM_{st} + bM_{Bd}) \\
&\qquad + \left\{R_p(1-\varphi)\left(\tau - \gamma\tau_1 + \frac{\gamma\tau_1\varphi}{1-\varphi}\right)\right. \\
&\qquad\quad \sum_{m=1}^{s} \frac{[B^*_{(r-1)}(s-m,b)]}{[B^*]}\theta e^{-\theta m} + R_p\varphi(1-\varphi) \\
&\qquad\quad \left. \times \beta \sum_{m=1}^{s} \frac{[B^*_{(r-1)}(s-m,b)]}{[B^*]}\theta^2 m e^{-\theta m} + R_p(1-\varphi)\gamma\tau_1\right.
\end{aligned}$$

$$\times \sum_{r_1=1}^{r-1} \sum_{b_1=1}^{b-1} \sum_{s_1+m=1}^{s} \frac{[\mathrm{B}^*_{(r-r_1-1)}(s-s_1-m, b-b_1)]}{[\mathrm{B}^*]}$$
$$\times \frac{[\mathrm{B}^*_{(r_1-1)}(s_1, b_1)]}{[\mathrm{B}^*]} \theta e^{-\theta m}$$
$$+ R_p(1-\varphi)^2 \frac{\beta}{2} \sum_{r_1=1}^{r-1} \sum_{b_1=1}^{b-1} \sum_{s_1+m=1}^{s} \frac{[\mathrm{B}^*_{(r-r_1-1)}(s-s_1-m, b-b_1)]}{[\mathrm{B}^*]}$$
$$\times \frac{[\mathrm{B}^*_{(r_1-1)}(s_1, b_1)]}{[\mathrm{B}^*]} \theta^2 m e^{-\theta m} \Bigg\} (sM_{st} + bM_{Bd}) V_R$$
$$r, s, b = 1, 2, 3, \ldots \tag{A.21}$$

where $(sM_{\mathrm{St}}+bM_{\mathrm{Bd}})$ is the molecular weight of $\mathrm{P}_{(r)}(s, b)$. The WCLD for the total copolymer can be obtained by adding together Eq. (A.21) over all r values, yielding

$$\frac{d}{dt}\{[\mathrm{P}(s, b)](sM_{\mathrm{St}} + bM_{\mathrm{Bd}})V_R\}$$
$$= -\Bigg\{\left[R_p V_R(1-\varphi)\left(\tau - \gamma\tau_1 + \beta\varphi + \frac{\gamma\tau_1\varphi}{1-\varphi}\right)\right]$$
$$+ [R_p V_R(1-\varphi)(\beta(1-\varphi) + 2\gamma\tau_1)]\Bigg\}$$
$$\times \frac{[\mathrm{B}^*(s, b)]}{[\mathrm{B}^*]} \times (sM_{\mathrm{St}} + bM_{\mathrm{Bd}})$$
$$+ \Bigg\{R_p(1-\varphi)\left(\tau - \gamma\tau_1 + \frac{\gamma\tau_1\varphi}{1-\varphi}\right) \sum_{m=1}^{s} \frac{[\mathrm{B}^*(s-m, b)]}{[\mathrm{B}^*]} \theta e^{-\theta m}$$
$$+ R_p\varphi(1-\varphi)\beta \times \sum_{m=1}^{s} \frac{[\mathrm{B}^*(s-m, b)]}{[\mathrm{B}^*]} \theta^2 m e^{-\theta m}$$
$$+ R_p(1-\varphi)\gamma\tau_1 \times \sum_{b_1=1}^{b-1} \sum_{s_1+m=1}^{s} \frac{[\mathrm{B}^*(s-s_1-m, b-b_1)]}{[\mathrm{B}^*]}$$
$$\times \frac{[\mathrm{B}^*(s_1, b_1)]}{[\mathrm{B}^*]} \theta e^{-\theta m}$$
$$+ R_p V_R(1-\varphi)^2 \frac{\beta}{2} \sum_{b_1=1}^{b-1} \sum_{s_1+m=1}^{s} \frac{[\mathrm{B}^*(s-s_1-m, b-b_1)]}{[\mathrm{B}^*]}$$
$$\times \frac{[\mathrm{B}^*(s_1, b_1)]}{[\mathrm{B}^*]} \times \theta^2 m e^{-\theta m} \Bigg\} (sM_{\mathrm{St}} + bM_{\mathrm{Bd}}) V_R$$
$$s, b = 1, 2, 3, \ldots \tag{A.22}$$